

Chapter 6

Design and implementation of a capacitive sensor system based on TiO₂ nanotubes for real time detection of methanol contamination in alcoholic beverages

6.1 Introduction

Alcoholic beverages are the complex mixture of alcohols, water, acids, mineral salts, sugars, aromatic compounds, etc. [1]. Out of all these compounds, ethanol is one of the most dominant component in any alcoholic beverages. However, contaminated alcoholic beverages majorly have an unsafe amount of methanol which severely damages human health [2]. Methanol usually produced by bacterial fermentation during alcohol production, for example, decomposition of aspartame (an artificial sweetener used in some beverages) and pectin (a naturally occurring fibre found in fruits) results in methanol production [1]. During distillation process, some part of the methanol gets distilled simultaneously with ethanol as methanol and ethanol both share similar kinds of physical and chemical properties [3].

As discussed in the introductory part of Chapter 1, in human body, methanol decomposes into toxic formaldehyde and formic acid which causes health problems like headache, fatigue, nausea, blurred vision and even death [4, 5]. Therefore, various countries and health agencies established a certain limit of permitted methanol content in these alcoholic beverages. As an example, European Union suggested any level above 10 gm methanol in 1 l of ethanol as unsafe [6]. WHO reported 500 mg/l of methanol concentration in blood results in toxicity whereas 1500-2000 mg/l can cause death [6]. Therefore, an efficient method for detecting methanol contamination in an alcoholic beverage is highly desirable.

In past, a number of following techniques have been used to find various contamination levels of methanol in alcoholic beverages: (i.) gas/liquid

chromatography [5], (ii.) sensor arrays [7], (iii.) near infrared spectroscopy [8], (iv.) Raman spectroscopy [9], (v.) optical sensor [10], and (vi.) Fourier transform infrared spectroscopy [11]. However, these techniques have a number of drawbacks i.e. (i.) not rapid results, (ii.) time consuming and complicated process involving sample preparation/pre-treatment, (iii.) problem of selectivity towards methanol with respect to ethanol when both VOCs exist in the sample, (iv.) sophisticated and costly measuring equipment, and (v.) complex post result analysis [1, 5]. In addition to this, irregularity in quality check, poor laboratory facilities and requirement of skilled manpower may instigate further setbacks. Therefore, a complete sensor system in product form which is simple, portable, fast, inexpensive and easy to operate is highly desirable.

TiO₂ is considered as one of the most chemically stable and environment friendly metal oxide nanomaterial [12, 17]. However, most of the reported TiO₂ based sensors are chemo-resistive in nature which exhibit poor selectivity [13]. Since, methanol and ethanol share a similar type of physical and chemical properties, therefore, it is difficult to use TiO₂ nanomaterial as a sensing layer for selective detection in chemo-resistive mode. Therefore, a new measurement technique was proposed for the selective detection of VOCs as discussed in Chapter 3. However, for achieving better selectivity towards methanol, the potentiality of TiO₂ nanotubes as a capacitive sensor was explored as sensitivity of the sensor depends upon the relative permittivity of analytes. Also, most of the reported work, in the past, lack in the details of sensor's interface with a signal processing circuit which limits its application in real time environment [17-19]. As an example, C. Wongchoosuk et al [19] reported sensor based on carbon nanotube-SnO₂ for detecting methanol contamination in whiskey but lacked the discussion about its implementation.

In this work, a capacitive type sensor system was developed which can detect 10-100% of methanol contamination in ethanol within 3 mins. Unlike discussed above conventional methods, this work is about developing a sensor system which is simple

to handle, reliable, fast, portable, and consume less power. This work reports the steps involved in the fabrication of sensor, the design of sensor system, and the implementation of sensor system in real-time environment. The sensor structure comprising of TiO₂ nanotubes array sandwiched in between two vertically placed electrodes. The sensor was tested in both controlled ambient and real-time environment situations for the following ambient: (i.) pure ethanol, (ii.) 10% methanol contaminated ethanol, (iii.) 25% methanol contaminated ethanol, and (iv.) pure methanol. Further, a signal processing circuit was designed for displaying (in the form of LEDs) methanol contamination level in the sample.

6.2 Experimental setup for VOC sensing

The details of the fabrication of TiO₂ nanotubes-based sensor was already discussed in sec. 2.2 (Chapter 2). For studying sensing properties, firstly, the sensor was placed inside a closed chamber and both resistive and capacitive responses of the sensor were measured for a precise concentration of 200 ppm of pure ethanol, pure methanol and methanol contaminated ethanol. Two terminals of the sensor were connected to an LCR meter and a 1V, 1 kHz AC signal was fed to the sensor through it. The change in resistance and capacitance value of the sensor was monitored simultaneously with a sampling rate of 3 readings per second. After getting maximum and saturated response, sensor was pulled out from the sensing chamber and placed in air ambient for the recovery of sensor. The temperature of the set-up was measured as 27 °C. Resistive and capacitive response of the sensor were measured upon exposure to 200 ppm of test vapors of (i.) pure ethanol, (ii.) 10% methanol in ethanol, (iii.) 25% methanol in ethanol, and (iv.) pure methanol. All the measurements were repeated minimum three times for each test vapors. The resistive (RRM) and capacitive (CRM) response magnitudes of the sensor were calculated by using eq. (2.1) and (2.2), respectively.

The sensor was then tested in real-time environment where the sensor was placed inside a glass bottle containing a solution having a mixture of different amounts of

ethanol and methanol. Finally, capacitive response of the sensor was tested for different levels of methanol contaminated whiskey samples for demonstrating the practical usage of the sensor system. Four different test alcohols (Table 6.1) of 10 ml each were poured into four different closed glass bottles (capacity= 250 ml). The fabricated sensor was then mounted inside the lid of the glass bottle and this lid was used to cover the above-mentioned bottles containing different test alcohols (Refer Fig. 6.2). Also, two terminals of the sensor were taken out from the lid and connected to an LCR meter for measuring capacitive change of the sensor upon exposure to different alcohols. For each run, the bottle was first covered by sensor mounted lid and after 150 s of exposure, the maximum capacitive change of the sensor was recorded. Then, the lid of the bottle was opened and the sensor was placed in air ambient for 250 s for recovery. To measure the repeatability of capacitive change of the sensor, the same procedure was replicated three times for all test VOCs

Table 6.1 Contents of the test samples.

<i>Sl. No.</i>	<i>Sample name (10 ml)</i>	<i>Ethanol (v/v)</i>	<i>Methanol (v/v)</i>
1	Ethanol	100%	0%
2	10% methanol	90%	10%
3	25% methanol	75%	25%
4	Methanol	0%	100%

For the next study, a commercially available whiskey was purchased from the general store which was prepared using scotch malt blended with grain spirits and had 42.8% of alcoholic contents. Three different samples of 10 ml were prepared as follows: (i.) pure whiskey, (ii.) 10% (v/v) methanol in whiskey, and (iii.) 25% (v/v) methanol in whiskey. The contents of pure whiskey and contaminated whiskey were further confirmed by using Gas Chromatography-Headspace (GC-HS) technique. For each bottle, the lid having sensor was used to cover bottle for 180 s and maximum

capacitance change of the sensor was observed. For the recovery of sensor, lid of the bottle was opened and placed in air ambient for 120 s. The same procedure was repeated three times for each bottle to measure the repeatability of the capacitive change of the sensor.

6.3 Design of the sensor system

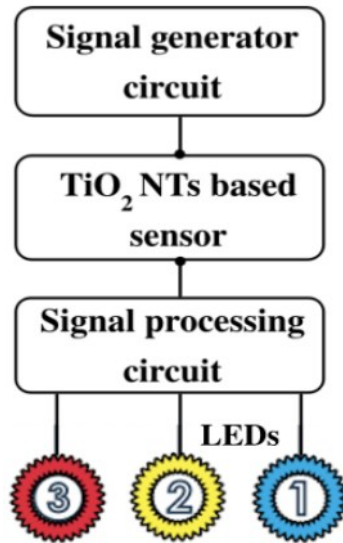


Fig. 6.1 Block diagram of the sensor system.

For realizing a portable sensor system, a signal processing circuit was designed and interfaced with the fabricated sensor device. A flow diagram and corresponding prototype of the sensor system are shown in Fig. 6.1 and Fig. 6.2, respectively. The sensor system has following three parts:

- i. Signal generator circuit: It comprises of an ICL8038 IC which generates a 1V, 1 kHz of an AC signal.
- ii. Signal processing circuit: This unit was made up of following components based on LM741 IC: (a.) A charge to voltage (Q-V) convertor was designed to get an output voltage proportional to the change in capacitance value of the sensor. (b.) In the next stage, a full-wave rectifier circuit was designed to convert AC output signal of Q-V convertor to an unregulated DC signal. (c.) Then, an RC low pass

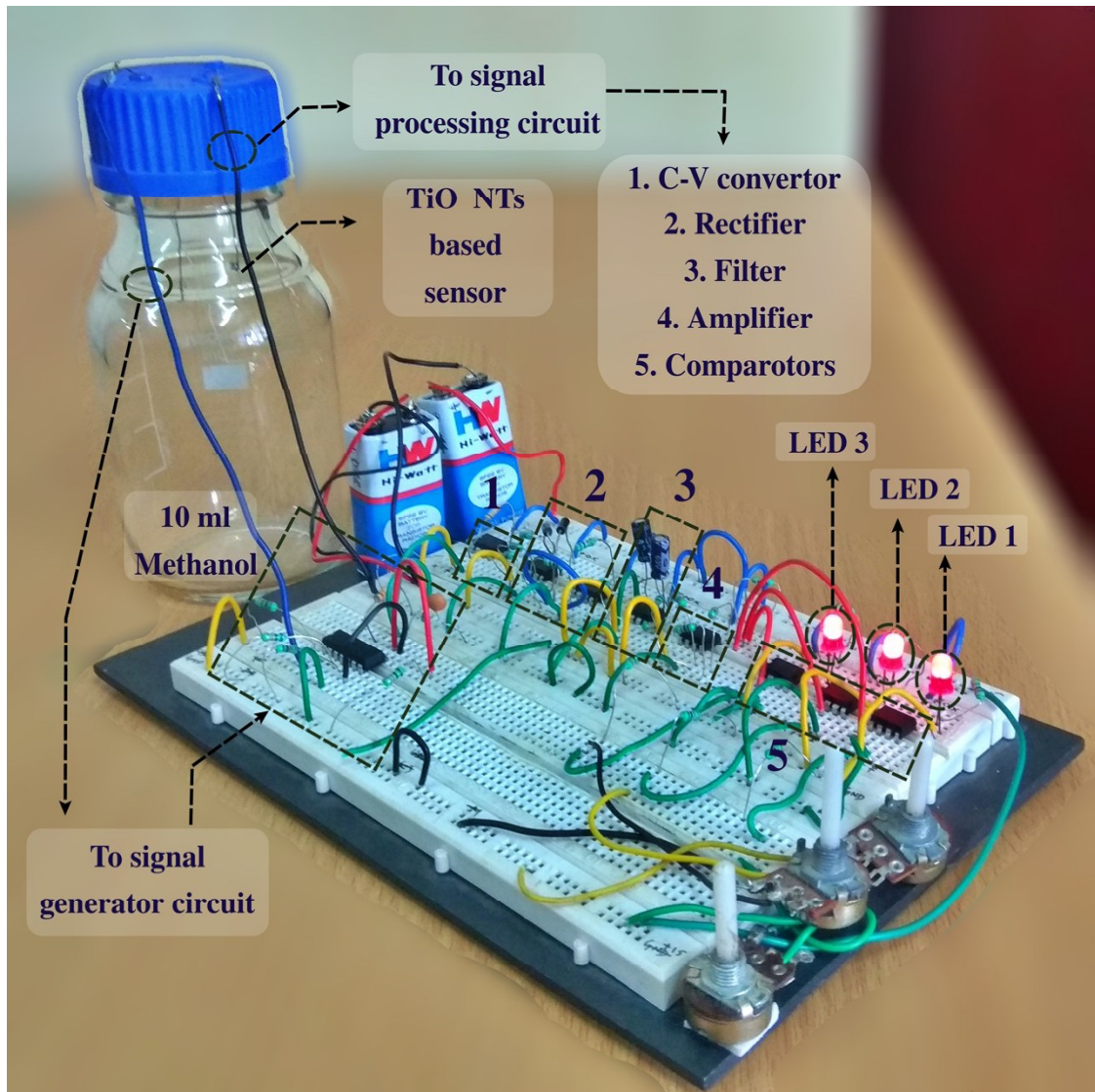


Fig. 6.2 Sensor system having sensor mounted inside a glass bottle and signal generator and processing circuit on bread board.

- filter was designed to get a regulated DC signal. (d.) In the next stage, LM741 IC was configured as an inverting amplifier to amplify and change the polarity of the DC signal. (e.) In the final stage, three comparators were used and their reference voltages were set with the help of a potential divider circuit having variable potentiometer. Three suitable reference voltages were set for determining three different contamination of methanol i.e. 10%, 25%, and 100%.
- iii. Sensor: Two terminals of the sensor were connected to the signal generator and processing circuit in the following way. One terminal of the sensor was connected

to the output pin of ICL8038 IC. The other terminal of the sensor was connected to the input of a signal processing unit which essentially detects capacitive change in the sensor and gives output in the form of a DC signal.

The sensor circuit system was operated using two 9 V alkaline batteries; thus, making the sensor system portable and easy to use. Fig. 6.2 represents the complete sensor system for detecting methanol contamination in alcoholic beverages. For testing the sensor system in real-time environment, the lid having sensor was used to cover four different bottles (250 ml) which had 10 ml of the following contents: (i.) Bottle 1 of pure whiskey, (ii.) Bottle 2 of 10% methanol contaminated whiskey, (iii.) Bottle 3 of 25% methanol contaminated whiskey and (iv.) Bottle 4 of pure methanol. For each bottle, the lid with sensor was used to cover bottle for 180 s and the output of all three LEDs were observed for getting the information about methanol contamination.

6. 4 Detection of methanol contamination using TiO₂ nanotubes based-sensor

Table 6.2 Resistive and capacitive sensing performance of the sensor in static mode.

<i>Alcohols (200 ppm)</i>	<i>Resistive sensing</i>			<i>Capacitive sensing</i>		
	<i>RRM (%)</i>	<i>Response time (s)</i>	<i>Recovery time (s)</i>	<i>CRM (%)</i>	<i>Response time (s)</i>	<i>Recovery time (s)</i>
Ethanol	97.2	572	1020	123	230	23
10% methanol	97.6	684	1052	234	385	24
25% methanol	98	714	1145	327	498	28
Methanol	99.1	610	1221	574	578	32

Fig. 6.3 (a) shows resistive response of the sensor upon exposure to 200 ppm of ethanol for three repeatable cycles. In the first cycle, it is evident from the graph that sensor was unable to recover to its baseline resistance completely in 10 mins and reached only up to 10.7 MΩ. In cycle 2, the resistance of the sensor, after recovery, was further decreased to 9.05 MΩ. Thus, sensor suffered from poor recovery characteristics when

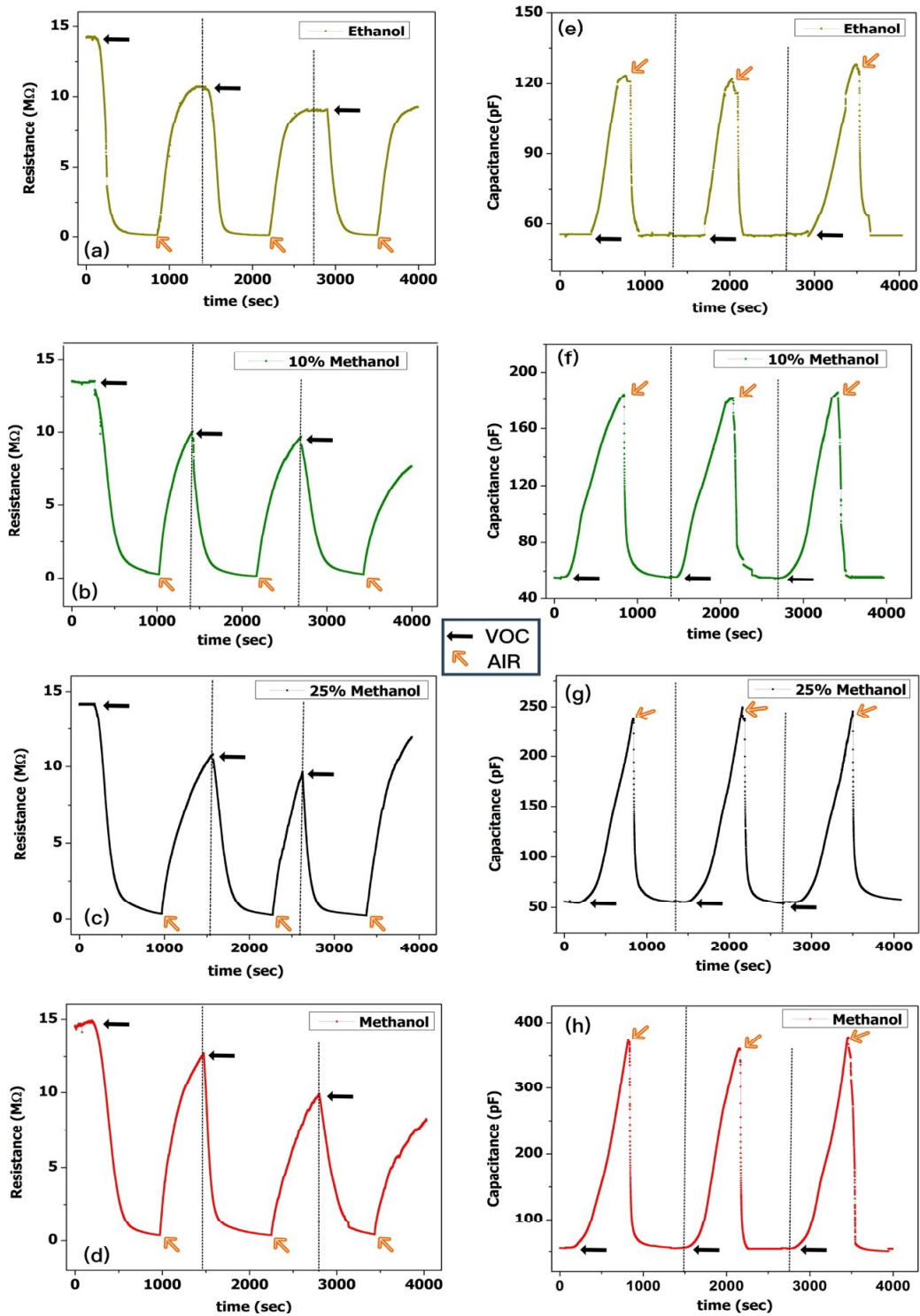


Fig. 6.3 Resistive response of the sensor upon exposure to 200 ppm of (a) ethanol, (b) 10% methanol contaminated ethanol, (c) 25% methanol contaminated ethanol, and (d) pure methanol. Capacitive response of the sensor upon exposure to 200 ppm of (e) ethanol, (f) 10% methanol contaminated ethanol, (g) 25% methanol contaminated ethanol, and (h) pure methanol.

operated in resistive mode at room temperature and needed more than 10 mins to recover to its original baseline resistance. After three cycles of response, the original baseline resistance was achieved by keeping the sensor in air ambient for 15 mins. The sensor was further exposed to 200 ppm of 10% methanol contaminated ethanol, 25% methanol contaminated ethanol and methanol as shown in Fig. 6.3 (b), (c) and (d), respectively. As evident, for all VOCs, the sensor was unable to recover to its baseline resistance value in 10 mins and a drift in baseline resistance was observed for repetitive cycles. Also, resistive response magnitude (RRM) of the sensor was calculated for four test samples (Table 6. 2) and found to be 97.2%, 97.6%, 98%, and 99.1% for ethanol, 10% methanol in ethanol, 25% methanol in ethanol and 100% methanol, respectively. It is evident from the above data that RRM was quite high for all the samples and the difference between RRM values of individual samples was negligible. Thus, TiO₂ nanotubes based sensor in resistive mode was unable to detect methanol contamination in ethanol.

Fig. 6.3 (e) shows the change in capacitance of the sensor upon exposure to 200 ppm ethanol for three repeatable cycles. In the first cycle, the capacitance of the sensor was increased from 55 pF to 123 pF. The sensor was able to recover to its baseline capacitance value within 40 s. Also, the sensor was able to recover to its baseline capacitance value repeatably within 1 min when exposed to 200 ppm of 10% methanol contaminated ethanol, 25% methanol contaminated ethanol and methanol as shown in Fig. 6.3 (f), (g) and (h), respectively. Thus, capacitive behaviour of the sensor exhibited efficient response/recovery kinetics with excellent repeatability towards all the four test samples. Most importantly, capacitive response magnitude (CRM) was found to be 123%, 234%, 327% and 574% for ethanol, 10% methanol in ethanol, 25% methanol in ethanol and 100% methanol, respectively. Thus, CRM of the sensor exhibited distinctive values for all four alcohols making the sensor selective for different levels of methanol contamination in ethanol. After the comparison of resistive and capacitive responses upon exposure to 200 ppm of pure ethanol, 10% methanol contaminated

ethanol, 25% methanol contaminated ethanol and pure methanol, it was found that the capacitive response displayed distinct responses for different ambient with better selectivity. Also, the sensor was able to recover to its baseline capacitance value with good repeatability. Thus, capacitive mode of the sensor was selected over conventional chemo-resistive mode for developing a sensor system to detect methanol contamination in alcoholic beverages.

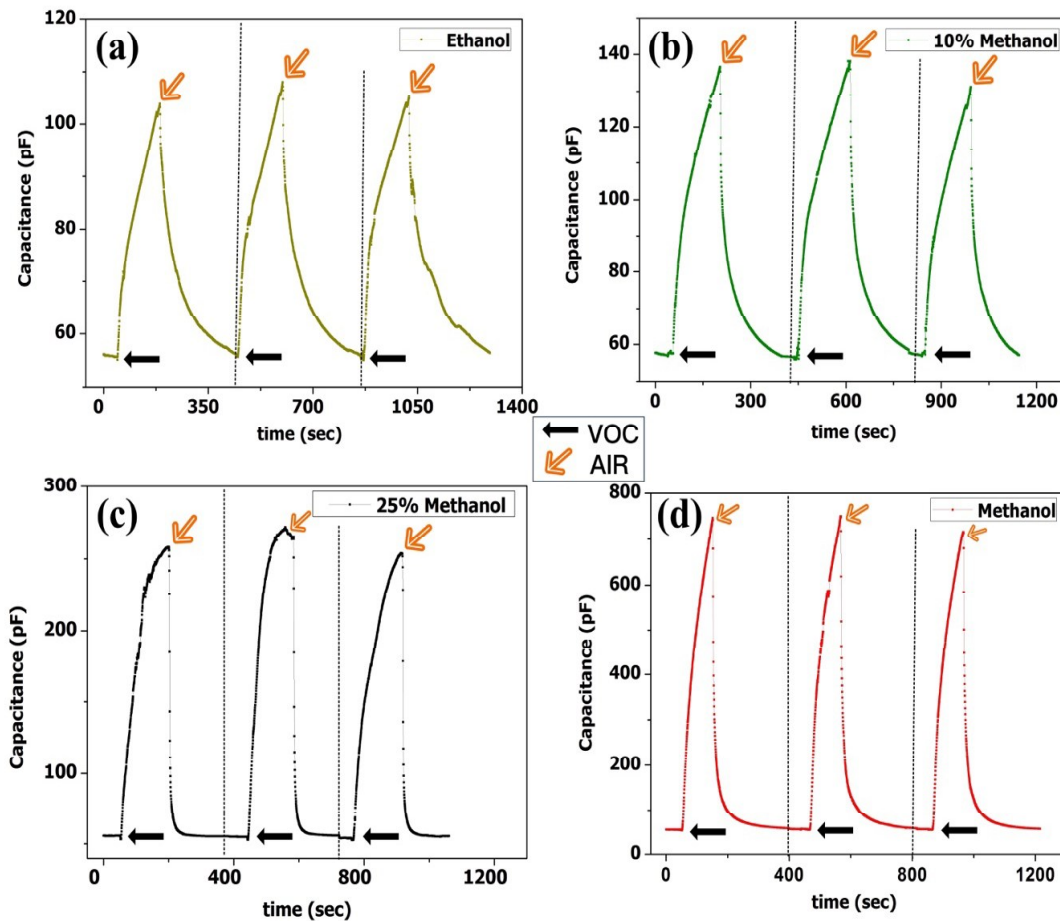


Fig. 6.4 Real environment capacitive response of the sensor placed in a 250 ml bottle having 10 ml of (a) ethanol, (b) 10% methanol in ethanol, (c) 25% methanol in ethanol, and (d) pure methanol.

Capacitive response of the sensor was tested in real-time environment ($\sim 27^\circ\text{C}$) when sensor was put inside four different glass bottles (250 ml each) containing 10 ml of four different methanol contaminated alcoholic solutions. Fig 6.4 (a) shows that

capacitance of the sensor was increased from 55 pF to 103 pF (CRM= 87.2%) when sensor was mounted inside a 250 ml bottle containing 10 ml of pure ethanol. Also, CRM of the sensor was found to be 145%, 389% and 1256% for 10% methanol contamination, 25% methanol contamination and pure methanol, respectively. Thus, it was found that sensor exhibited the least capacitive response towards ethanol and response was increased with increase in methanol concentration. Therefore, the sensor exhibited excellent selectivity property by discriminating methanol and ethanol when operated in capacitive mode. Also, the sensor exhibited excellent repeatability for all alcoholic solutions and was able to achieve its baseline capacitance value within 40 s for each cycle.

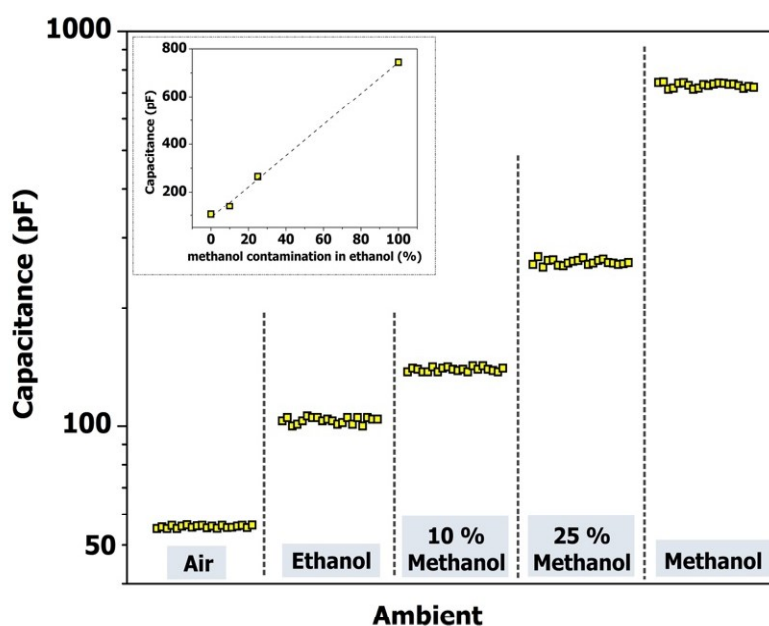


Fig. 6.5 Scattered plot showing various repetitive capacitance values of the sensor when placed in 250 ml of bottle having air, 10 ml of ethanol, 10 ml of 10% methanol contaminated ethanol, 10 ml of 25% methanol contaminated ethanol, and 10 ml of pure methanol.

Fig. 6.5 shows a scattered plot of the capacitance of the sensor when placed in air ambient and in above mentioned ambient and the results displayed excellent repeatability and relatively distinctive values of the capacitances for different ambient. Inset of Fig. 6.5 shows typical capacitance values of the sensor for different levels of

methanol contaminated ethanol. Due to the discriminating and repeatable nature, the sensor system proved its suitability to detect $>10\%$ and $<25\%$ of methanol contamination in ethanol with high accuracy.

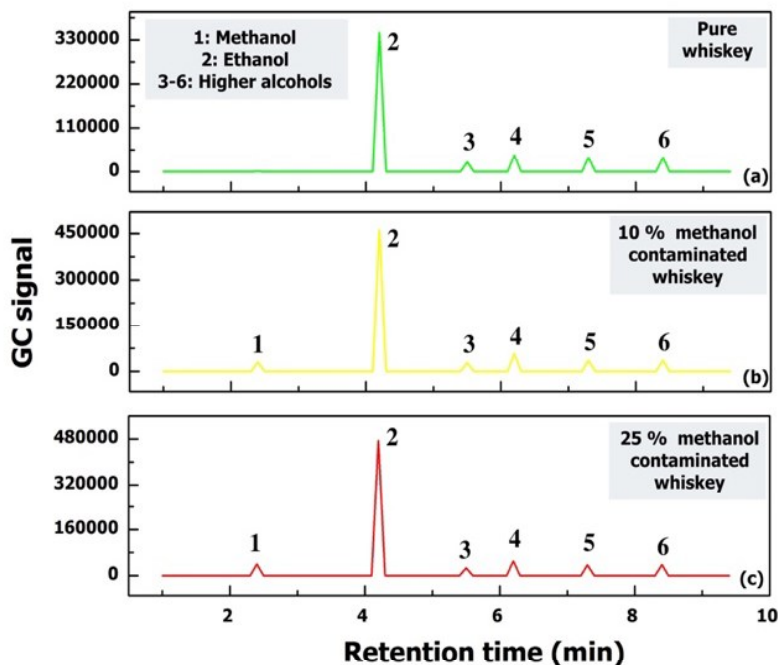


Fig. 6.6 GC-HS spectra of (a) pure whiskey, (b) 10% methanol contaminated whiskey, and (c) 25% methanol contaminated whiskey.

Fig. 6.6 (a-c) shows the peaks obtained from the GC-HS of pure whiskey, 10% methanol contaminated whiskey, and 25% methanol contaminated whiskey, respectively. Pure whiskey sample shows no methanol peaks, however, for 10% methanol contamination, a peak just before ethanol peak was detected and this peak became more dominant for 25% methanol contaminated whiskey sample. The capacitive responses of the sensor in presence of pure and methanol contaminated whiskey were tested further and results are shown in Fig. 6.7. Capacitive response of the sensor in presence of pure whiskey gave a tiny response but increased with the percentage of methanol contamination in whiskey. The sensor operating at room temperature exhibited fairly distinct capacitive response for ethanol and methanol contaminated ethanol. These results were in accordance with the above discussed

results as the sensor exhibited the least capacitive change for ethanol and the most for methanol.

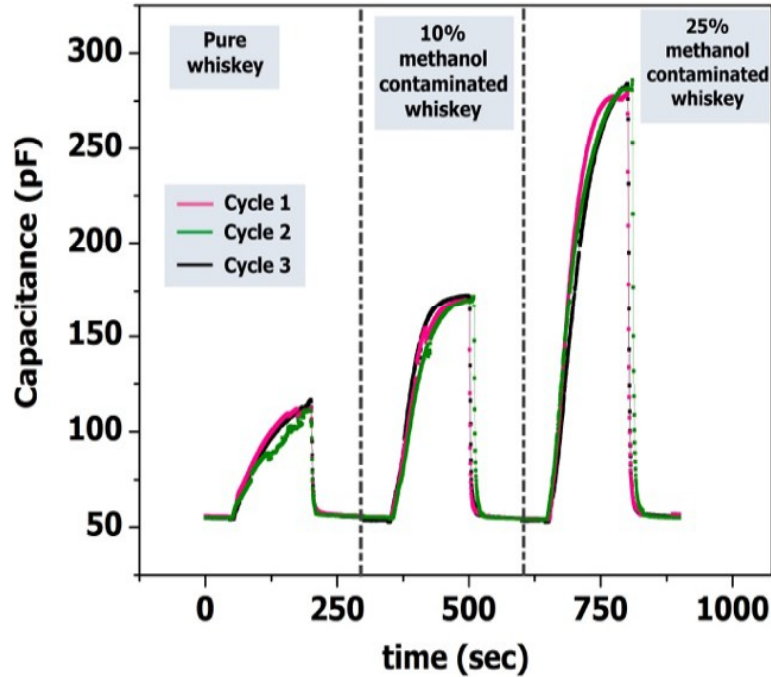


Fig. 6.7 Capacitive response of the sensor when placed in 250 ml of bottle containing 10 ml of (a) pure whiskey, (b) 10% methanol contaminated whiskey, and (c) 25% methanol contaminated whiskey.

After studying the capacitive response of the sensor in both controlled and real-time ambient by using an LCR meter, the sensor was then connected to a portable signal processing circuit as shown in Fig. 6.2. Different capacitive changes of the sensor were converted into respective voltage signals by using a charge to voltage (Q-V) converter circuit. Thus, different capacitances correspond to different voltages and these voltage changes were detected by a three-comparator circuit. The output of each comparator was connected to an LED as shown in Fig. 6.2. No LED was ON in pure ethanol or pure whiskey ambient. The output of first comparator became high when 10% methanol contamination was detected and LED 1 became ON as a notification. Similarly, the output of both first and second comparators became high when 25% methanol contamination was detected by the sensor system and both LEDs (1 and 2)

got ON as a notification. Lastly, the output of all three comparators became high when 100% methanol was detected by the circuit and all three LEDs (1, 2 and 3) got ON as a notification.

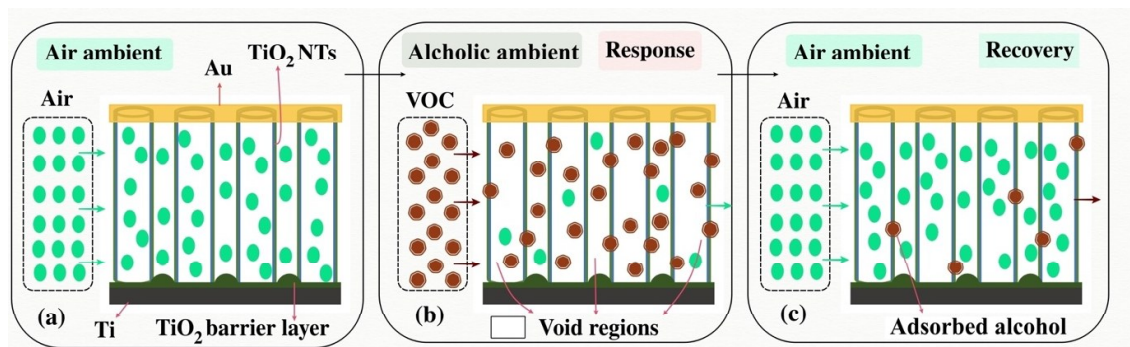


Fig. 6.8 Schematics of the Au/TiO₂ nanotubes/Ti based sensor showing (a) equilibrium state in air ambient, (b) sensor response in alcohol ambient, and (c) sensor recovery in air ambient.

The general sensing mechanism for TiO₂ nanotubes based sensor for VOC detection was already discussed in sec. and 2.5 (Chapter 2) and 3.6 (Chapter 3). With reference to these discussions, this section explains the advantages of using capacitive sensor over resistive sensor for detecting methanol contamination in ethanol by discussing sensing mechanism of the sensor. Fig. 6.8 (a) shows a schematic of the sensor when placed in air ambient. As evident, the space between two electrodes of the sensor filled with either void regions (major volume) or TiO₂ nanotubes. In alcohol ambient, the alcoholic molecules get adsorbed on the inner and outer surface of TiO₂ nanotubes and void regions get filled through diffusion as shown in Fig. 6.8 (b). Thus, resistance of the sensor changes when target molecules react with the adsorbed oxygen ions. Different organic vapors react with these surface ions with different rates and different resistance changes were observed in dissimilar ambient. However, since, ethanol and methanol exhibit similar types of chemical properties, the resistive change of the device exhibited almost similar values, and thus it results in the poor selectivity of the sensor. On the contrary, the capacitive mode of the sensor depends upon tracking change in the value of dielectric constant of the medium when sensor gets exposed to

different organic compounds. Upon exposure to different target alcohols, the dielectric property of the sensor gets changed. Since, the dielectric constant of methanol ($\epsilon_r = 32.7$) is different compared to ethanol ($\epsilon_r = 24.5$), the sensor in capacitive mode was able to discriminate between different methanol contamination levels in ethanol successfully showing better selectivity compared to resistive mode.

Fig. 6.8 (c) represents the recovery of the sensor when placed in air ambient just after alcohol ambient. At room temperature, the sensor in resistive mode does not get enough desorption energy to recover. Thus, the sensor displayed a lethargic recovery to its baseline resistance (Ref. Fig. 6.3 (a-d)). On the other hand, free space between two electrodes which was previously filled by diffused alcohol molecules get instantly replaced by air due to higher concentration gradient, and thus sensor was recovered to its baseline capacitance value as soon as the medium between two electrodes was changed to air. Therefore, the capacitive mode of TiO₂ nanotubes based sensor exhibited improved selectivity and faster response/recovery than resistive mode even at room temperature.

6.5 Conclusions

In this chapter, TiO₂ nanotubes based parallel plate sensor and its signal processing unit were developed for the detection of methanol contamination in ethanol based alcoholic beverages. The sensor was tested both in conductive and capacitive mode at room temperature for 200 ppm of pure ethanol, 10% methanol contaminated ethanol, 25% methanol contaminated ethanol and pure methanol. Resistive response of the sensor exhibited high but very similar response magnitudes towards all the four alcoholic samples with recovery time >10 mins. On the other hand, the capacitive response was distinct for different samples with very fast recovery (<1 min). Methanol contamination in commercial whiskey was also detected successfully by the developed capacitive sensor. Finally, TiO₂ nanotubes based capacitive sensor was integrated with a battery driven signal processing unit making the system portable, simple to handle

and economical. The developed sensor system has the potential to monitor methanol content while distilling alcoholic beverages and to ensure the quality of the distilled alcohol.

References

1. C.Y. Zhang, N.B. Lin, X.S. Chai, Z Li, D.G. Barnes, A rapid method for simultaneously determining ethanol and methanol content in wines by full evaporation headspace gas chromatography, *Food Chem.* 183 (2015) 169-172.
2. W.B. Yant, H.H. Schrenk, R.R. Sayers, Methanol antifreeze and methanol poisoning, *Ind. Eng. Chem.* 23 (1931) 551-555.
3. R.E. De Góes, L.V.M. Fabris, M. Muller, J.L. Fabris, Light-assisted detection of methanol in contaminated spirits, *J. Light. Technol.* 3 (2016) 4499-4505.
4. C. Md, T. Elena, F. Ibolya, F. Erzsébet, A survey on the methanol content of home distilled alcoholic beverages in Transylvania (Romania), *Acta Medica Marisiensis* 59 (2014) 206-208.
5. M.L. Wang, J.T. Wang, Y.M. Choong, Simultaneous quantification of methanol and ethanol in alcoholic beverage using a rapid gas chromatographic method coupling with dual internal standards, *Food Chem.* 86 (2004) 609-615.
6. E.I. Ohimain, Methanol contamination in traditionally fermented alcoholic beverages: the microbial dimension, *SpringerPlus* 5 (2016) 1607.
7. N.A. Beckers, M.T. Taschuk, M.J. Brett, Selective room temperature nanostructured thin film alcohol sensor as a virtual sensor array, *Sensors and Actuators B* 176 (2013) 1096-1102.
8. H.L. Fernandes, I.M.R. Jr, C. Pasquini, J.J.R. Rohwedder, Simultaneous determination of methanol and ethanol in gasoline using NIR spectroscopy: Effect of gasoline composition, *Talanta* 75 (2008) 804-810.
9. I.H. Boyaci, H.E. Genis, B. Guven, U. Tamer, N. Alper, A novel method for quantification of ethanol and methanol in distilled alcoholic beverages using Raman spectroscopy, *J. Raman Spectrosc.* 43 (2012) 1171-1176.
10. B. Kieser, F. Dieterle, G. Gauglitz, Discrimination of methanol and ethanol vapors by

- the use of a single optical sensor with a microporous sensitive layer, *Anal. Chem.* 74 (2002) 4781-4787.
11. J.M. Garrigues, A. Perez-Ponce, S. Garrigues, M. de la Guardia, Direct determination of ethanol and methanol in liquid samples by means of vapor phase-Fourier transform infrared spectrometry, *Vibrational Spectroscopy* 15 (1997) 219-228.
 12. H. Zhang, J.F. Banfield, Structural characteristics and mechanical and thermodynamic properties of nanocrystalline TiO₂, *Chemical Reviews* 114 (2014) 9613-9644.
 13. J. Bai, B. Zhou, Titanium dioxide nanomaterials for sensor applications, *Chemical Reviews* 114 (2014) 10131-10176.
 14. G. Chen, S. Ji, H. Li, X. Kang, S. Chang, Y. Wang, G. Yu, J. Lu, J. Claverie, Y. Sang, H. Liu, High-energy faceted SnO₂-coated TiO₂ nanobelt heterostructure for near-ambient temperature-responsive ethanol sensor, *ACS Appl. Mater. Interfaces* 7 (2015) 24950-24956.
 15. A. Nikfarjam, S. Hosseini, N. Salehifar, Fabrication of a highly sensitive single aligned TiO₂ and gold nanoparticle embedded TiO₂ nano-fiber gas sensor, *ACS Appl. Mater. Interfaces* 9 (2017) 15662-15671.
 16. A.V. Raghu, K.K. Karuppanan, B. Pullithadathil, Highly Sensitive, temperature-independent oxygen gas sensor based on anatase TiO₂ nanoparticle grafted 2D mixed valent VO_x nanoflakelets, *ACS Sensors* 3 (2018) 1811-1821.
 17. Z. Lou, F. Li, J. Deng, L. Wang, T. Zhang, Branch-like hierarchical heterostructure (α -Fe₂O₃/TiO₂): a novel sensing material for trimethylamine gas sensor, *ACS Appl. Mater. Interfaces* 5 (2013) 12310-12316.
 18. J. Nisar, Z. Topalian, A.D. Sarkar, L. Österlund, R. Ahuja, TiO₂-based gas sensor: a possible application to SO₂, *ACS Appl. Mater. Interfaces* 5 (2013) 8516-8522.
 19. C. Wongchoosuk, A. Wisitsoraat, A. Tuantranont, T. Kerdcharoen, Portable electronic nose based on carbon nanotube-SnO₂ gas sensors and its application for detection of methanol contamination in whiskeys, *Sensors and Actuators B* 147 (2010) 392-399.
 20. Y. Li, D. Deng, X. Xing, N. Chen, X. Liu, X. Xiao, Y. Wang, A high performance methanol gas sensor based on palladium-platinum-In₂O₃ composited nanocrystalline SnO₂, *Sensors and Actuators B* 237 (2016) 133-141.



This document was created with the Win2PDF “print to PDF” printer available at <http://www.win2pdf.com>

This version of Win2PDF 10 is for evaluation and non-commercial use only.

This page will not be added after purchasing Win2PDF.

<http://www.win2pdf.com/purchase/>